EARTHQUAKE OBSERVATIONS AND ANALYSES OF A NUCLEAR POWER PLANT

Shin-ichi Hirashima(I), Muneaki Kato(II), Teruyuki Ueshima(III)

SYNOPSIS

Observations of earthquakes indicate that structures on large foundation mats receive less intensity in high-frequency range (Ref. 1, 2). The same phenomenon was recognized in earthquake observations of a nuclear reactor building. Conveniently, forced vibration tests on this building resulted the simulated mathematical models (Ref. 3). Studies using the models showed that the input effective wave for response analyses closely resemble the observed wave at the foundation. The effective wave could be worked out sufficiently from the observed wave at the free field surface by Dr. H. Yamahara's theory. The most suitable filtering constant was 0.23 sec.

INTRODUCTION

The nuclear reactor building described in this paper is that of Tokai No. 2 Nuclear Power Plant, Tokai Village, Ibaraki Prefecture, Japan. This plant (1100 MWe, BWR-MARK 2) has been generating electric power commercially since 1978.

EARTHQUAKE OBSERVATIONS

The epicentral distance of the earthquake which was observed on June 12, 1978 was about 250 km and its intensity was 7.4 in terms of magnitude. Seismic records were obtained on three floors of the reactor building and at two points of the adjacent soil 140 m apart from the building (Fig. 1). The recorded acceleration time histories indicate that building motions apparently have less intensities than soil motions in high-frequency range (Fig. 2). The calculated amplification ratios of the observed foundation motions to the soil motions are compared with the theoretical transfer functions by Yamahara's equation Eq. (1), (Fig. 3). The transfer functions of the foundation relative to the soil surface showed almost complete agreement in case of $\tau = 0.23$ second in Eq. (1). The transfer functions of the foundation relative to the bedrock did not show very good agreement.

$$\eta = (\sin \epsilon) / \epsilon \qquad \cdots\cdots\cdots\cdots\cdots\cdots (1)$$

where

η : transfer function
ϵ : $\pi f \tau$
f : frequency in Hz
τ : filtering constant in sec

The wave (C) calculated from the observed soil surface motion (A) by Eq. (2) is compared with the observed foundation motion (B) (Fig. 4) and their velocity response spectra are compared (Fig. 5). The waves (B) and (C) are very similar. Filtered waves (F, G) determined from the bedrock motions do not agree

(I) Shimizu Construction Co., Ltd., Tokyo, Japan
(II) The Japan Atomic Power Company, Tokyo, Japan
(III) Central Research Institute of Electric Power Industry, Civil Engineering Laboratory, Japan

very well with the observed foundation motion (E) (Fig. 6, Fig. 7).

$$U_t = \frac{1}{n} \sum_{i=-(n-1)/2}^{(n-1)/2} u_t + i\Delta t \qquad \cdots\cdots\cdots\cdots\cdots\cdots (2)$$

where

U_t: filtered wave
u_t: soil motion
Δt: time interval
$n = \tau / \Delta t$

FORCED VIBRATION TEST

The forced vibration test at the plant were performed in Febrary 1977. Their results have been reported (Ref. 3). Results relevant to this paper are transcribed here. Two large vibrator units forced the operating floor of the reactor building horizontally in a direction of south and north (Fig. 8). Each unit, capable of exciting maximum horizontal force of 150 tons, was controlled at a force amplitude level of about 30 tons and the responses of the buildings and soil were recorded with resonance amplitudes and phases at 0.1 Hz pitch from 1 Hz to 20 Hz. The recorded resonance displacements are compared with the calculated resonance curves appling the simulated models (Fig. 9).

The simulated mathematical model RS in Fig. 10 has the physical constants in Table 1 and thus the damped eigenvalues in Table 3. The other simulated model RTS in Fig. 11 has the constants in Table 2 and thus the damped eigenvalues in Table 4. The model type RTS was created in order to be able to make simulations considering the cross-interaction effects between the reactor building and the adjacent turbine building. RTS resulted in a second resonance peak being at about 3.5 Hz, the same as with the observed resonance curves. However, RS did not have this second peak. Therefore, it is certain that this second peak suggests the cross-interaction effect. Simplified cross-interaction equations are given as Eq. (3) concerning Fig. 12. The theoretical solutions for "$_0k_{ii}$" have been well known as one of the soil-structure problems (Timoshenko, Barkan, Tajimi, and others). The other constants "$_0k_{ij}$" are the stiffness expressing the cross-interaction effects and their theoretical solutions were worked out for RTS (Ref. 4). Rocking and vertical motions couple with each other as shown in Fig. 13 and their mathmatical models can be represented as Fig. 14.

$$\left.\begin{aligned} \delta_1 &= \delta_{11} + \delta_{21}, \quad \delta_{11} = P_1 / {}_0k_{11}, \quad \delta_{21} = P_2 / {}_0k_{21} \\ \delta_2 &= \delta_{12} + \delta_{22}, \quad \delta_{12} = P_2 / {}_0k_{12}, \quad \delta_{22} = P_2 / {}_0k_{22} \end{aligned}\right\} \cdots\cdots\cdots\cdots\cdots (3)$$

EFFECTIVE INPUT WAVE FOR RESPONSE ANALYSIS

Calculated seismic response waves applying the simulated model RTS are compared with the observed seismic waves (Fig. 15), when the observed earthquake record of the foundation was used for the input wave in the calculation. They agree with each other fairly well. It is important that the calculated response wave of the foundation closely resembles the input wave. On the other hand, the mathematically

filtered soil surface motions closely resemble the observed foundation motions. These facts indicate that the effective wave for earthquake response analyses can be obtained from soil surface motions by the method of mathematical filtering. The seismic design values of the reactor building are compared with the values calculated from the simulated models of the forced vibration tests (Fig. 16). The seismic design of the reactor building may be in a fully safer side.

CONCLUDING REMARKS

The effective input earthquake wave for the reactor building could be calculated from soil surface motions, but not from bedrock motions. The satisfactory value of the smoothing filter constant "τ" obtained was 0.23 sec, higher than values reported previously regarding a number of ordinary buildings. We think that soil-foundation side interaction is important in the mechanism of effective wave formation and further studies are needed to explain for the mechanism clearly.

The work reported herein was accomplished under the suggestions of Dr. K. Akino[II] and Dr. H. Yamahara[I].

REFERENCES

1. H. Yamahara, "Ground Motions during Earthquakes and the Input Loss of Earthquake Power to an Excitation of Buildings", Soil and Foundations, Vol. 10, No. 2, pp. 145-161, Tokyo, 1970.

2. N. M. Newmark, W. J. Hall and J. R. Morgan, "Comparison of Building Response and Free Field Motion in Earthquakes", 6th WCEE, Vol. 2, pp. 972-978, New Delhi, 1977.

3. M. Kato, A. Kato, K. Hanada and S. Hirashima, "Forced Vibration Tests at the Tokai No. 2 Nuclear Power Plant, Part 1-3", 5th JEES, pp. 1449-1472, Tokyo, 1978. (in Japanese)

4. S. Hirashima, "A Study on Dynamic Analyses of Nuclear Reactor Buildings", Reports of the Research Laboratory of Shimizu Construction Co., Ltd., Vol. 29, pp. 51-62, Tokyo, 1978. (in Japanese)

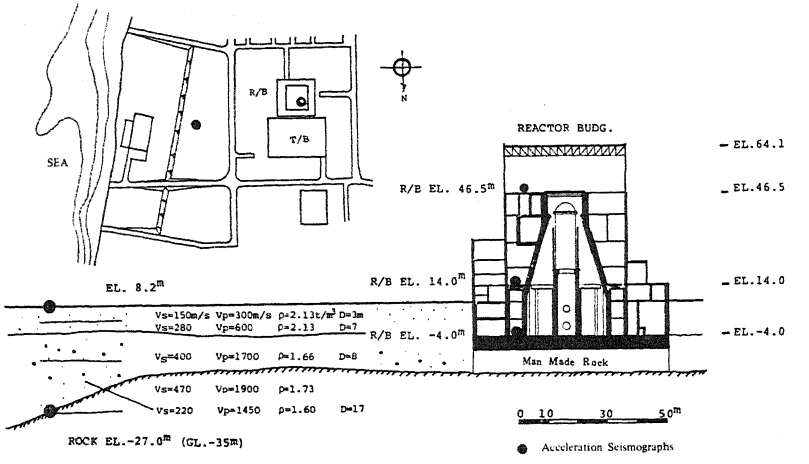

Fig. 1 Location of Seismographs at the Tokai No.2 Nuclear Power Plant

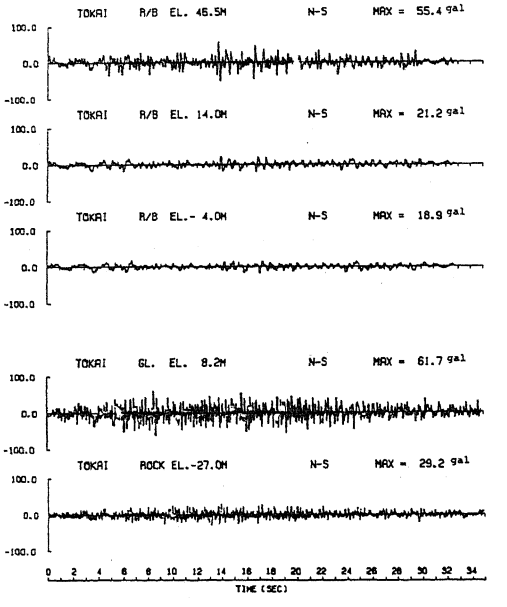

Fig. 2 Observed Acceleration Waves

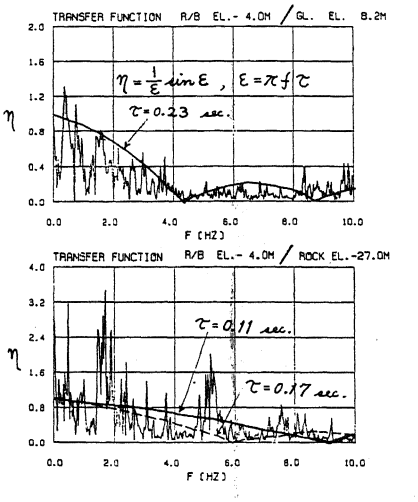

Fig. 3 Comparison of Transfer Functions (Foundation/Soil) Determined from Observed Records and from Eq. (1)

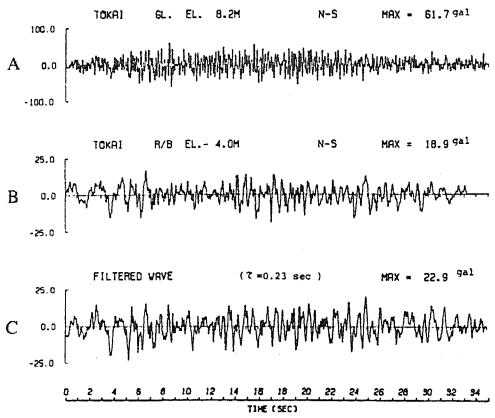

Fig. 4 Observed Records and Filtered Wave

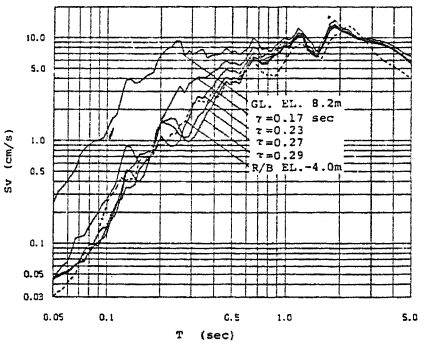

Fig. 5 Velocity Response Spectrua of Observed Records and Filtered Waves

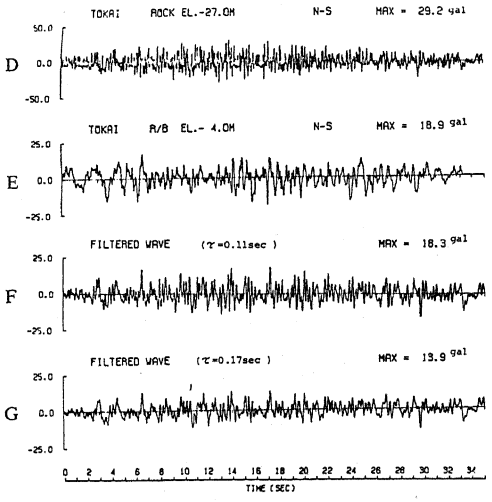

Fig. 6 Observed Records and Filtered Waves

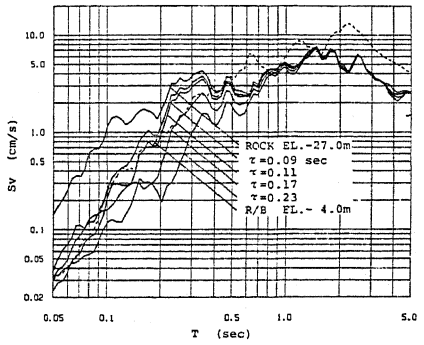

Fig. 7 Velocity Response Spectrua of Observed Records and Filtered Waves

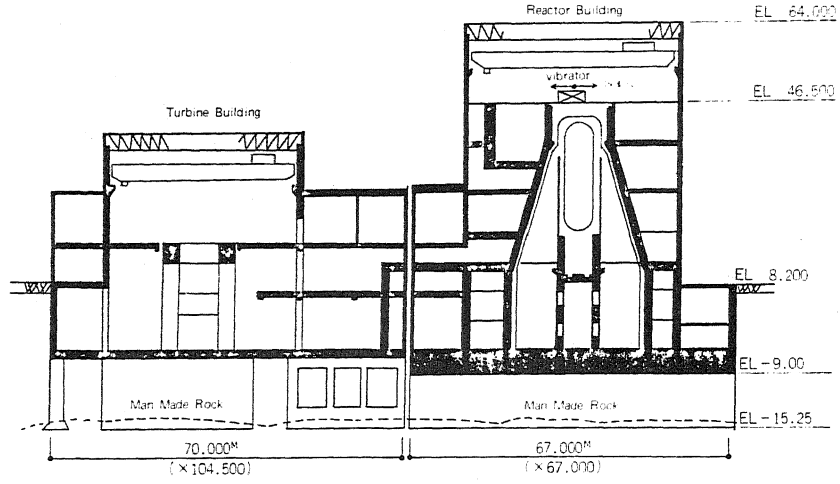

Fig. 8 Cross Section of Reactor Building and Turbine Building

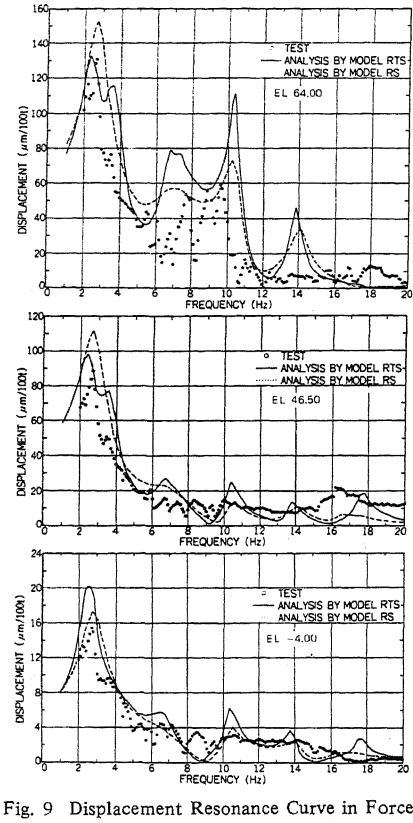

Fig. 9 Displacement Resonance Curve in Forced Vibration Tests

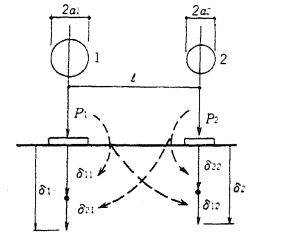

Fig. 12 Simplified Cross- interaction

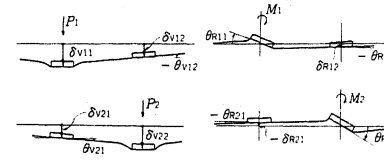

Fig. 13 Rotation and Vertical Motion

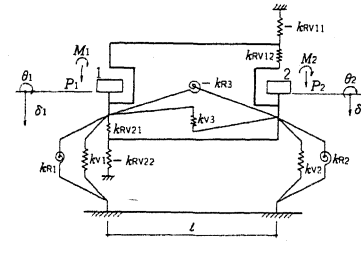

Fig. 14 Mathematic Model of Fig. 13

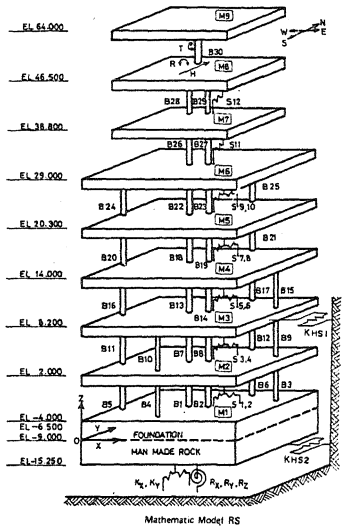

Fig. 10 Simulated Mathmatic Model RS applied to Forced Vibration Tests

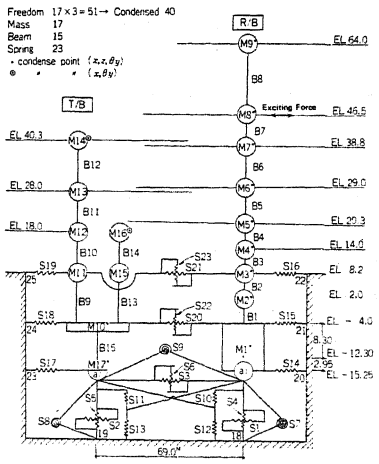

Fig. 11 Simulated Mathematic Model RTS

Table 1 Physical Constants of RS

MASS ELEMENT						
Mn	Weight (t)	Gravity center (m) X	Y	Weight moment (×10³ tm²) Ix	Iy	Iz
M1	143,988	33.1	32.9	564.25	540.30	1104.55
M2	18,539	33.1	35.0	87.00	84.97	171.97
M3	23,403	35.6	33.7	108.07	108.19	216.26
M4	21,945	37.5	37.1	77.45	79.86	157.31
M5	17,941	31.2	37.1	65.90	85.70	151.60
M6	16,151	30.6	36.3	50.30	47.70	98.00
M7	16,040	31.7	34.5	25.00	17.99	42.99
M8	10,267	32.7	35.5	20.98	21.18	42.16
M9	3,419	32.0	33.5	9.52	8.52	18.04

BEAM ELEMENT						
Bn	Position (m) X	Y	Shear section area (m²) y	x	Sect. mo. of ina. (×10³m⁴) J_z	J_y	J_x
B1	32.0	32.0	83.1	83.1	36.10	18.00	18.00
B2	32.0	33.5	271.2	206.6	115.70	64.80	72.40
B3	67.0	33.5	100.5	0.0	0.00	0.00	37.60
B4	33.5	0.0	0.0	100.5	0.00	37.60	0.00
B5	0.0	33.5	100.5	0.0	0.00	0.00	37.60
B6	33.5	67.0	0.0	100.5	0.00	37.60	0.00
B7	32.0	32.0	83.1	83.1	36.10	18.00	18.00
B8	32.0	33.5	227.1	190.5	115.70	64.80	72.40
B9	67.0	33.5	100.5	0.0	0.00	0.00	37.60
B10	33.5	0.0	0.0	100.5	0.00	37.60	0.00
B11	0.0	33.5	100.5	0.0	0.00	0.00	37.60
B12	33.5	67.0	0.0	100.5	0.00	37.60	0.00
B13	32.0	32.0	83.1	83.1	36.10	18.00	18.00
B14	32.0	33.5	260.8	190.1	115.70	64.80	72.30
B15	67.0	31.4	78.4	0.0	0.00	0.00	30.80
B16	0.0	47.0	33.3	0.0	0.00	0.00	5.30
B17	33.5	67.0	0.0	83.8	0.00	37.60	0.00
B18	32.0	32.0	80.3	80.3	29.20	14.60	11.60
B19	32.0	33.5	163.3	119.6	77.12	43.20	48.30
B20	0.0	46.6	31.0	0.0	0.00	0.00	5.11
B21	12.5	67.0	0.0	19.1	0.00	1.24	0.00
B22	32.0	32.0	72.6	72.6	19.90	9.97	9.97
B23	32.0	33.5	117.9	162.2	69.40	38.90	43.40
B24	0.0	46.6	31.0	0.0	0.00	0.00	5.11
B25	22.3	67.0	0.0	43.3	0.00	6.63	0.00
B26	32.0	32.0	57.7	57.7	9.87	4.93	4.93
B27	32.0	33.5	83.9	73.9	46.30	25.90	28.90
B28	32.0	32.0	174.5	77.4	14.73	0.28	22.62
B29	32.0	33.5	67.6	56.8	33.07	28.17	31.37
B30	32.0	33.5	27.1	25.3	24.98	23.74	26.43

INTERACTION					
Horizontal	Kx, Ky	1.57×10⁷ t/m	Ec = 235 t/cm²		h = 1 %
	Ma	73502 t	Qc = 100 t/cm²		
	Tx, Ty	0.0481 s	Rock.	Rx, Ry	1.47×10¹⁰ t·m
	K_{HS1}	0.306×10⁷ t/m		Is	5.54×10⁷ t·m²
	T_{HS1}	0.0497 s		Tr	0.0302 s
	K_{HS2}	0.460×10⁷ t/m	Tort.	Rt	3.6×10¹⁰ t·m
	T_{HS2}	0.0385 s		Is	3.15×10⁷ t·m²
				Tr	0.0331 s

Table 2 Physical Constants of RTS

MASS ELEMENT			
No.	weight (t)	weight moment (×10⁶t·m²)
M 1*	143,989	564.25
M 2	18,539	87.00
M 3	23,403	108.07
M 4	21,945	77.45
M 5	17,941	65.90
M 6	16,151	50.30
M 7	13,540	25.00
M 8	10,267	20.98
M 9	3,419	9.52
M10*	89,330	392.7
M11	35,970	188.1
M12	25,070	177.63
M13	9,198	65.26
M14	5,465	11.84
M15	400	1.57
M16	11,750	2.908
M17*	62,280	272.8
a_1	130,573	1285
a_2	34,833	538
$\frac{1}{2}$B15	62,280	272.8

M 1*=M 1+a_1
M10*=M10+$\frac{1}{2}$B15
M17*=M17+a_2

BEAM ELEMENT				
No.	shear sect. (㎡)	sec. area (㎡)	sect. mo. of ina. (×10⁴m⁴)	damp. h_B (%)
B 1	555.3	823.8	165.6	1
B 2	511.2	823.8	165.6	1
B 3	455.6	656.4	136.4	1
B 4	274.6	391.0	60.01	1
B 5	221.5	367.0	58.48	1
B 6	141.6	247.7	33.83	1
B 7	242.1	360.4	53.99	1
B 8	27.1	52.4	26.43	1
B 9	344.0	636.0	120.8	1
B10	188.0	378.0	25.06	1
B11	127.0	237.0	34.59	1
B12	30.0	113.0	6.675	1
B13	146.0	175.0	4.743	1
B14	142.0	170.0	4.743	1
B15	7,315.0	7,315.0	2990	16

B1~B7, B9~B14: E=294t/cm², G=125t/cm²
B 8: E=210t/cm², G=90t/cm²
B15: E=4.79t/cm², G=1.65t/cm²
γ=t/K

SPRING ELEMENT			
No.	stiff. (×10⁶t/m) (×10⁶t·m)	damping h_K(%)	γ (S/%)
S 1	111	1	3.25
S 2	27.7	1	4.48
S 3	19.6	1	0
S 4	122	1	6.94
S 5	30.9	1	7.67
S 6	13.7	1	0
S 7	25.2	1	1.44
S 8	12.5	1	0.77
S 9	− 5.3	1	0
S10	2.85	1	0
S11	2.85	1	0
S12	− 3.9	1	0
S13	− 5.9	1	0
S14	26.5	1	1.15
S15	21.5	1	2.96
S16	6.71	1	4.93
S17	26.5	1	1.15
S18	21.5	1	2.96
S19	6.71	1	4.93
S20	28.5	1	0
S21	28.5	1	0
S22	0.274	1	0
S23	0.274	1	0

Table 3 Damped Eigenvalues of RS

n	natura. freq. (Hz)	modal damp. f.	modal parti. f.
1, 2	2.91	0.256	−0.240±0.235 i
3, 4	5.05	0.671	0.0418∓0.0144 i
5, 6	7.11	0.198	0.105±0.745 i
7, 8	10.41	0.044	0.203∓0.861 i

Table 4 Damped Eigenvalues of RTS

n	natura. freq. (Hz)	modal damp.f.	modal parti.f.
1, 2	1.733	0.321	−0.00305±0.00512 i
3, 4	2.391	0.145	−0.00756∓0.02383 i
5, 6	2.556	0.214	−0.11017±0.09779 i
7, 8	2.866	0.554	−0.00232∓0.01133 i
9, 10	3.663	0.147	−0.04525±0.21765 i
11, 12	4.399	0.259	−0.02135∓0.02905 i
13, 14	6.918	0.097	0.13387±0.66065 i
15, 16	7.101	0.027	0.14641∓0.06089 i
17, 18	7.904	0.076	0.08701∓0.14686 i
19, 20	7.983	0.147	−0.07386∓0.05805 i
21, 22	10.43	0.030	−0.00274∓1.0190 i
23, 24	10.50	0.141	0.00226±0.00434 i
25, 26	10.68	0.034	0.09741∓0.22258 i

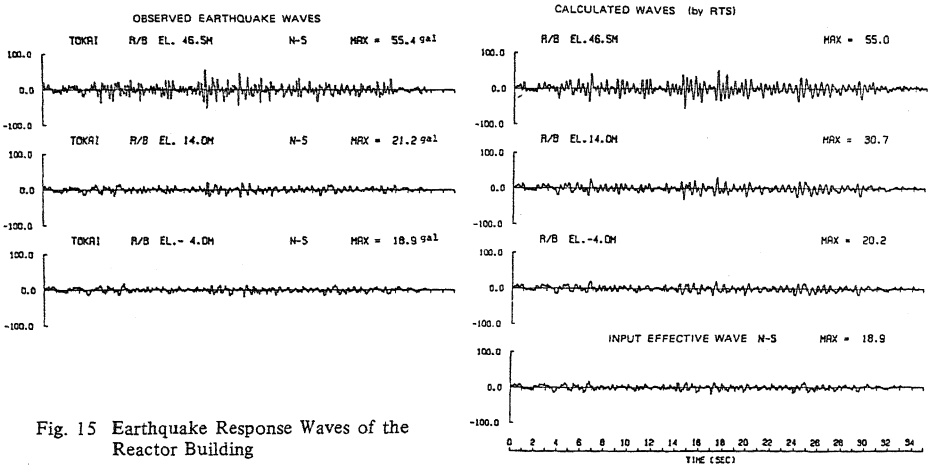

Fig. 15 Earthquake Response Waves of the Reactor Building

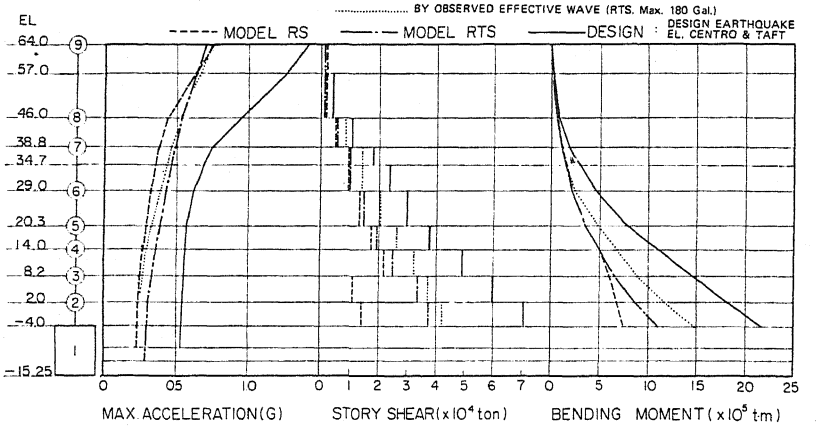

Fig. 16 Comparison of Maximum Responses Obtained from Simulated Models and Seismic Design Values